Spectroscopic Characterization of an Fe^{IV} Intermediate Generated by Reaction of XO^- (X = Cl, Br) with an Fe^{II} Complex Bearing a Pentadentate Non-Porphyrinic Ligand − Hydroxylation and Epoxidation Activity

Véronique Balland,[a] Marie-France Charlot,[b] Frédéric Banse,*[b] Jean-Jacques Girerd,*[b] Tony A. Mattioli,[a] Eckhard Bill,[c] Jean-François Bartoli,[d] Pierrette Battioni,[d] and Daniel Mansuy[d]

Keywords: Iron / Oxo ligands / Bioinorganic chemistry / Epoxidation / Hydroxylation

Mononuclear Fe^{IV} intermediates have been generated in MeOH upon reaction of sodium hypochlorite or hypobromite with a ferrous complex bearing the pentadentate ligands *N*-methyl-*N*,*N*′,*N*′-tris(2-pyridylmethyl)ethane-1,2-diamine (L_5^2) or *N*-methyl-*N*,*N*′,*N*′-tris(2-pyridylmethyl)propane-1,3-diamine (L_5^3). These highly unstable green complexes are characterized by an absorption band at ca. 750 nm. Mössbauer data indicate that the iron center is low spin (S = 1) with an axial electronic structure, allowing identification of the mononuclear Fe^{IV} complexes as $[L_5Fe^{IV}O]^{2+}$ or $[L_5Fe^{IV}OCH_3]^{3+}$. In acetonitrile/dichloromethane solutions, the $L_5^3Fe^{IV}$ system exhibits very selective activities toward hydroxylation of cyclohexane or epoxidation of cyclooctene and *cis*-stilbene. Computational studies performed on $[L_5Fe^{IV}O]^{2+}$ and on the model compound $[(NH_3)_5Fe^{IV}O]^{2+}$ reveal that the ground state possesses two unpaired electrons in the two π^* orbitals, as known for O_2. Electronic spectra computed by time-dependent DFT exhibit only one band in the visible region that is essentially due to d-d transitions.

Introduction

Porphyrinic Fe^{IV}−oxo species have been detected by spectroscopy in several heme enzymes[1−7] and their chemical models.[8−11] With respect to non-heme enzymes, studies of Fe^{IV} species are more recent and thus less advanced. Dinuclear $Fe^{III}Fe^{IV}$ or $Fe^{IV}Fe^{IV}$ species have been identified in enzymes[12,13] as well as having been chemically modeled.[14−18] The mononuclear non-heme Fe^{IV}−oxo entity has frequently been postulated in the catalytic cycle of enzymes[19,20] but to date has not been characterized. From reactivity studies of chemical models, Que et al. have postulated mononuclear Fe^{IV}−oxo intermediates.[21] Using macrocyclic tetraamido ligands, mononuclear Fe^{IV}−Cl and Fe^{IV}−CN species have been prepared and studied by Collins et al.[22,23] To the best of our knowledge, the first spectroscopic study of a non-heme mononuclear Fe^{IV}−oxo species was reported by Grapperhauser et al.[24] This complex was obtained with the macrocyclic tetraamino ligand cyclam-acetato. With the ligand tetramethylcyclam (TMC), Rohde et al. very recently obtained the complex $[Fe^{IV}(O)(TMC)(NCCH_3)]^{2+}$ after reaction of iodosylbenzene or H_2O_2 with a ferrous precursor in CH_3CN at −40 °C.[25] Moreover, they were able to obtain its X-ray crystallographic structure, since the species is stable at −40 °C in CH_3CN for at least one month. With the tetradentate tripodal ligand TPA [tris(2-pyridylmethyl)amine)], the same authors obtained the intermediate $[Fe^{IV}(O)(TPA)]^{2+}$.[26] Owing to its relative instability, the latter complex is a more efficient oxygen-atom transfer agent than $[Fe^{IV}(O)(TMC)(NCCH_3)]^{2+}$.

In this paper, we report the preparation and spectroscopic characterization of an Fe^{IV}−oxo (or methoxo) species in methanol with a non-porphyrinic nonmacrocyclic ligand as well as the preliminary study of the reactivity of the Fe^{IV}−oxo form in acetonitrile/dichloromethane.

Our strategy was to use a pentadentate ligand leaving one vacant site on the Fe center which could potentially be occupied by an oxygen species. This allowed us, and others in the past, to obtain low-spin $Fe^{III}OOH$ species.[27−34] For

[a] Laboratoire de Biophysique du Stress Oxydant, SBE/DBJC CEA/Saclay,
91191 Gif-sur-Yvette, France
[b] Laboratoire de Chimie Inorganique, UMR CNRS 8613, Université Paris-Sud,
91405 Orsay, France
[c] Max-Planck-Institut für Strahlenchemie,
45470 Mülheim an der Ruhr, Germany
[d] Chimie et Biochimie Pharmacologiques et Toxicologiques, UMR CNRS 8601, Université René Descartes (Paris V),
45 Rue des Saints-Pères, 75270 Paris cedex 06, France
Supporting information for this article is available on the WWW under http://www.eurjic.org or from the author.

instance, the $Fe^{III}OOH$ species was obtained by addition of an excess of H_2O_2 to $[L_5{}^2Fe^{II}Cl]^+$.[27,30,31,35]

In the same manner, we prepared a low-spin $Fe^{III}OOH$ species with $L_5{}^3$.[36]

In order to generate an $Fe^{IV}O$ entity we adopted the strategy of studying the reaction of the oxygen atom donors ClO^- or BrO^- with $[L_5{}^3Fe^{II}Cl]^+$ and $[L_5{}^2Fe^{II}Cl]^+$ (Scheme 1).

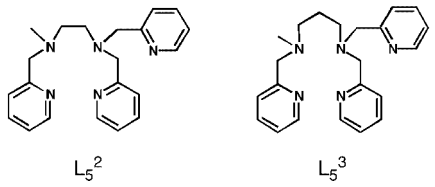

Scheme 1. Pentadentate ligands used in this study

Results and Discussion

UV/Vis Spectroscopy

The reaction of $[L_5{}^3Fe^{II}Cl]PF_6$ at −50 °C in CH_3OH with 2 equiv. of ClO^- was monitored by UV/Vis spectroscopy. Visually, a transient orange color first appeared which quickly changed to green. The green solution exhibited a band at 742 nm which persisted for about 5 min. In Mössbauer samples, this green species correspond to almost 70% of the total Fe. Taking into account the loss of this unstable species upon transfer to the Mössbauer cell, one can assume that in the solution used for UV/Vis spectroscopy, the conversion is almost quantitative. The extinction coefficient is thus $\varepsilon \approx 300\ M^{-1}cm^{-1}$.

The reaction in CH_3OH at 0 °C between $[L_5{}^3Fe^{II}Cl]PF_6$ and 100 equiv. of ClO^- was monitored by stopped-flow UV/Vis spectroscopy (Figure 1).

The maximum intensity of the band at 742 nm was obtained after 100 ms. It completely disappeared under these conditions after 2.5 s. The absorption maximum for the initial orange species was detected at 430 nm and at 0 °C it disappeared in 50 ms.

The same reaction was studied starting from $[L_5{}^2Fe^{II}Cl]PF_6$ and the series of spectra for the first 200 ms is shown in Figure 1. Even though the spectral features are very similar, some differences between the $L_5{}^2$ and $L_5{}^3$ complexes can be noted. The initial absorption band, corresponding to the orange complex, lies at 440 nm. This complex is less fleeting than its $L_5{}^3$ analog since the 440-nm band was still observable as a shoulder after 200 ms. This orange species evolved to the green complex as a clear isobestic point was observed at 503 nm. The green species was characterized by a band at 756 nm with a maximum absorbance weaker than the one observed for the $L_5{}^3$ analog, suggesting a lower conversion into the green species for the $L_5{}^2$ system. This last observation is consistent with the fact that the orange and green complexes coexist in solution in the $L_5{}^2$ system. Finally, the reactivities of $[L_5{}^3Fe^{II}Cl]PF_6$ and $[L_5{}^2Fe^{II}Cl]PF_6$ in the presence of ClO^- are similar but the stabilities of the green and orange species are different.

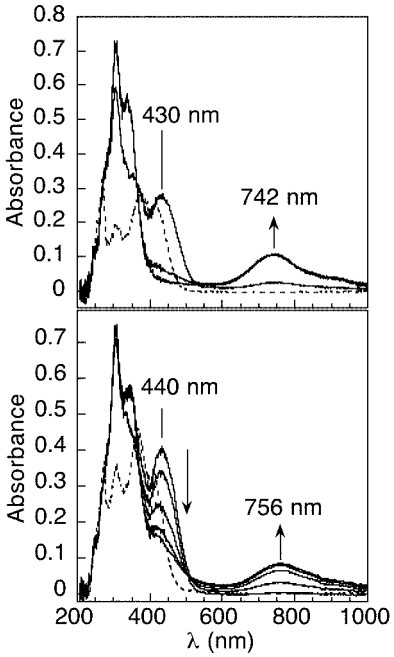

Figure 1. Evolution of the reaction between 0.5 mM $[L_5{}^3Fe^{II}Cl]PF_6$ (top) or $[L_5{}^2Fe^{II}Cl]PF_6$ (bottom) and 100 equiv. of ClO^- monitored in CH_3OH at 0 °C by stopped-flow absorption spectroscopy; the evolutions are shown between 0 and 100 ms for $L_5{}^3$ and 0 and 200 ms for $L_5{}^2$; the spectra in dashed lines are relative to the Fe^{II} starting complexes (0.5 mM)

By ozonolysis of a ferric complex with the ligand cyclamacetato, Grapperhauser obtained an $Fe^{IV}=O$ complex, characterized by a green colour (λ_{max} = 676 nm).[24] The complex $[Fe^{IV}(O)(TMC)(NCCH_3)]^{2+}$ reported by Rohde et al.[25] was also characterized by a pale green colour, with an absorption maximum at 820 nm and an extinction coefficient of 400 $M^{-1}cm^{-1}$. By using the ligand TPA, Lim and co-workers[26] were able to prepare an $Fe^{IV}=O$ complex in CH_3CN at −40 °C. This pale green intermediate exhibited a band at 724 nm with an extinction coefficient of ca. 300 $M^{-1}.cm^{-1}$. These characteristics are similar to the ones observed in the present study.

Mössbauer Spectroscopy

For Mössbauer studies a sample was prepared from $[L_5{}^3Fe^{II}Cl]PF_6$ labeled with 50% ^{57}Fe. The complex was oxidized with 2 equiv. of ClO^- at −60 °C and the green solution thus obtained was quickly frozen to 77 K.

In the absence of an applied magnetic field, the oxidation product exhibited an asymmetric quadrupole doublet at 80 K that could be deconvoluted in two symmetric subspectra. The isomer shift and quadrupole splitting of the minor species [$\delta(2) = 0.35\ mm{\cdot}s^{-1}$, $\Delta E_Q(2) = 0.88\ mm{\cdot}s^{-1}$] indicate the presence of some oxidized Fe^{III} contaminant,[37] whereas the major sub-spectrum (1) can be assigned to the green oxidation product (68% relative abundance, determined from the magnetic spectra given below). The parameters $\delta(1) = 0.02\ mm{\cdot}s^{-1}$ and $\Delta E_Q(1) = 1.20\ mm{\cdot}s^{-1}$ are indicative of low-spin Fe^{IV} species.[38]

Applied field measurements show that the major component (1) in fact possesses integer spin. Weak fields (1 T) at 4.2 K induce only weak magnetic splittings due to the nuclear Zeeman effect resulting from the applied field (Figure 2, top), but the internal fields are vanishingly small according to dominating strong zero-field splittings (zfs) and an $M_S = 0$ ground level without significant level mixing. Sizeable internal fields were detected only at strong fields (7 T) and higher temperatures. In contrast, the contaminating species sub-spectrum (2) shows a wide magnetically split hyperfine pattern due to half-integer spin or even magnetic ordering. The large splittings attenuate the absorptions of this minor contribution to an almost vanishing baseline distortion.

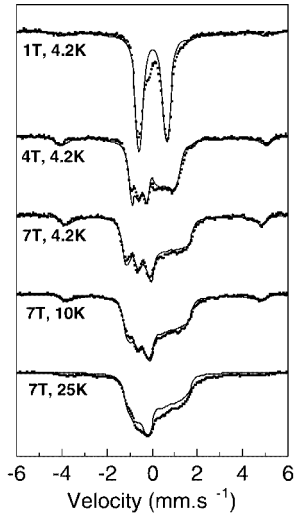

Figure 2. Mössbauer spectra of ^{57}Fe-enriched $[L_5{}^3Fe^{II}Cl]PF_6$ + 2 equiv. of ClO^- recorded at variable fields and temperatures; simulations of the spectra, made by considering a low-spin mononuclear Fe^{IV} complex, are represented by solid lines; the contamination background [sub-spectrum (2), 32% relative intensity] was taken into account by a simulation based on the equation given in the text for $S = 5/2$, $\delta = 0.4$ mm·s^{-1}, $\Delta E_Q = 0.7$ mm·s^{-1}, $D = 1$ cm^{-1}, $E/D = 0.33$, $A'_{iso}/g_N\beta_N = -19$ T

The field and temperature dependence of the magnetic Mössbauer spectra of the green oxidation product could be well simulated using the usual spin Hamiltonian

$$H = D\,[S_z{}^2 - 2/3 + E/D\,(S_x{}^2 - S_y{}^2)] + \mu_B\,\mathbf{B}\,g\,\boldsymbol{S} + H_N$$

for an electronic spin $S = 1$, where D and E/D are the zfs parameters, and H_N is the usual nuclear Hamiltonian for the ^{57}Fe nucleus.[39] The values of the spin Hamiltonian and hyperfine parameters are summarized in Table 1. We mention that alternative fits with $S = 2$ required magnetic hyperfine coupling constants with a small isotropic contribution $A'_{iso}/g_N\beta_N = -6.5$ T which is unreasonable and far below the values for known high-spin Fe^{IV}, $S = 2$, compounds.[22,40,41] This implies that the green oxidation product is an $S = 1$ species like the known oxo−ferryl compounds.

The values obtained for the green complex generated by reaction of $[L_5{}^3FeCl]^+$ with 2 equiv. of ClO^- compare well with those reported for the complexes obtained with the non-heme ligands of the cyclam family[24,25] or the amine/pyridine ligand TPA[26] (see Table 1). The Mössbauer parameters are also similar to those reported for the compound I analogue $S = 1$ Fe^{IV}=O derivative of Fe−porpholactone $[Fe^{IV}$=O**2**$]^+$.[10] For Horse Radish Peroxidase compound II, it was found that $\delta = 0.03$ mm/s and $\Delta E_Q = 1.61$ mm/s.[3] The Mössbauer analysis for the $S = 1$ porphyrinic dimethoxy complex $[Fe^{IV}(TMP)(OCH_3)_2]$ gave $\delta = -0.025$ mm/s and $\Delta E_Q = 2.1$ mm/s.[42,43] The $Fe^{IV}{}_2O_2$ diamond-core complex involving two $S = 1$ metal centers recently characterized by the group of Que yielded corresponding values for δ (0.1 mm/s) and ΔE_Q (1.75 mm/s).[18] These comparisons demonstrate that the parameters obtained from Mössbauer analysis are similar for all the Fe^{IV} species with oxygenated ligands and are independent of the nuclearity of the moieties and of the environment(s) of the metal ion(s). In contrast, low-spin $Fe^{IV}-CN$[23] and $Fe^{IV}(CN\,tBu)_2$[44] species have much larger ΔE_Q values (4.35 mm/s and 3.38 mm/s) although the δ values are similar. This strongly suggests that the $L_5{}^3Fe^{IV}$ complex has an oxygenated group as an axial ligand. The small E/D value observed here is also consistent with an axial electronic structure. This is confirmed a contrario by the larger E/D value (0.15) found by Que et al. for the dinuclear $Fe^{IV}{}_2O_2$ complex. We propose, therefore, that the green species in MeOH can be formulated as an oxo species $[L_5{}^3Fe^{IV}O]^{2+}$ or its methoxo derivative $[L_5{}^3Fe^{IV}OCH_3]^{3+}$.

We suggest that the orange species, which absorbs at 430 nm, could be the ClO^- adduct. This complex then ev-

Table 1. Mössbauer parameters obtained for several mononuclear Fe^{IV} complexes; the formulae used for the ligands are given according to the references cited

Ligand	$L_5{}^3$	TMC[25]	Cyclam-acetato[24]	**2**$^{2-}$ [10]	TPA[26]
δ [mm/s]	0.03	0.17	0.01	0.08	0.01
ΔE_Q [mm/s]	1.21	1.24	1.37	1.66	0.92
η	0.53	0.5	0.8	0.3	0.9
D [cm^{-1}]	22.5	29	23	20	28
E/D	0.01	0	0	0.1	0
g_x, g_y, g_z	2, 2, 2	2.3, 2.3, 2	2, 2, 2	2.17, 2.17, 1.99	
$A/g_N\beta_N$ [T]	−18, −20.6, −0.4	−22.5, −18, −3	−23, −23, −10	−17.5, −17.5, −10	−23.5, −23.5, −5

olves to the high-valent iron complex characterized by an absorption band at 742 nm. The observed events can thus be summarized as shown in Scheme 2.

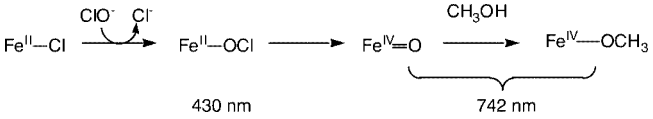

Scheme 2. Mechanism proposed for the formation of mononuclear Fe^{IV} complexes from ClO^- and $[L_5{}^3Fe^{II}Cl]^+$ or $[L_5{}^2Fe^{II}Cl]^+$

Resonance Raman Spectroscopy

We recorded resonance Raman spectra of the green species (prepared with either $Br^{16}O^-$ or $Br^{18}O^-$ in a 25 mM solution of the complex in MeOH/acetone, 2:1) using excitation at 752.5 nm and acetone was used in order to increase the solubility of the complex. In both cases, the green species was characterized by the same UV/Vis spectrum as the one observed using ClO^-. The Raman spectrum is shown in Figure 3 and the band at 752 cm^{-1} is a good candidate for the $Fe^{IV}-$oxygen vibration. Indeed, its frequency is similar to the ones reported for several ferryl−oxo heme proteins.[45] Moreover, this is the only band of the spectrum that vanishes when the green colour disappears. However, no shift was observed upon ^{18}O labelling. It is possible that either a fast exchange between $[L_5{}^3Fe^{IV}O]^{2+}$ and unlabelled H_2O occurred as reported for the intermediate ES of cytochrome c peroxidase[46,47] or that the green intermediate in the presence of methanol is an $Fe^{IV}OCH_3$ species.[48]

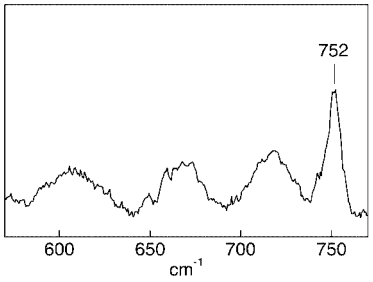

Figure 3. Resonance Raman spectrum at 10 K of the Fe^{IV} green complex prepared with a 25 mM solution of $[L_5{}^3Fe^{II}Cl]PF_6$ in presence of BrO^-; the laser wavelength used was 752.5 nm

In the case of the complex $[Fe^{IV}(O)(TMC)(NCCH_3)]^{2+}$,[25] no $Fe^{IV}=O$ vibration could be detected by Raman spectroscopy using laser excitation at 752.5 nm. However, this vibration was detected at 834 cm^{-1} by Fourier transform IR spectroscopy. With porphyrinic ligands, the $Fe^{IV}-$oxo vibration frequencies are greater than 800 cm^{-1}.[49,50] Complementary studies are therefore necessary to unambiguously assign the 752 cm^{-1} vibration observed here.

Reactivity

Reactivity studies were conducted at −20 °C with 2 equiv. of ClO^- in a mixture of acetonitrile/dichloromethane, 1:1, under aerobic conditions for cyclohexane and cyclooctene and under argon for *cis*-stilbene. The solution was stirred for 3 h and the products analyzed (Table 2).

Table 2. Yields (%/ClO^-) obtained at −20 °C for the oxidation reactions of different substrates by $[L_5{}^3FeCl]PF_6$ + 2 equiv. of ClO^- (Bzl = benzaldehyde, 800 equiv. of substrate)

Cyclohexan-		-cyclooctene		-Stilbene	
-ol	-one	Epoxy-	*cis*-	*trans*-	Bzl
10	0	15	0	10	0

The $[L_5{}^3FeCl]PF_6/ClO^-$ mixture is able to hydroxylate cyclohexane in 10% yield relative to the oxidant. Remarkably no ketone was formed. This high selectivity towards hydroxylation indicates the absence of free radical chemistry since the oxidation is performed under aerobic conditions.[51] Cyclooctene was epoxidized in a 15% yield, which is comparable to the yield of 30% reported for the intermediate $[Fe^{IV}(O)(TPA)]^{2+}$.[26] Epoxidation of *cis*-stilbene occurred with a 10% conversion but with a complete isomerization to the *trans*-epoxide. Such an isomerization has been attributed to a long-lived radical as observed with heme $Fe^{IV}=O$ species.[52] This is illustrated in Scheme 3.

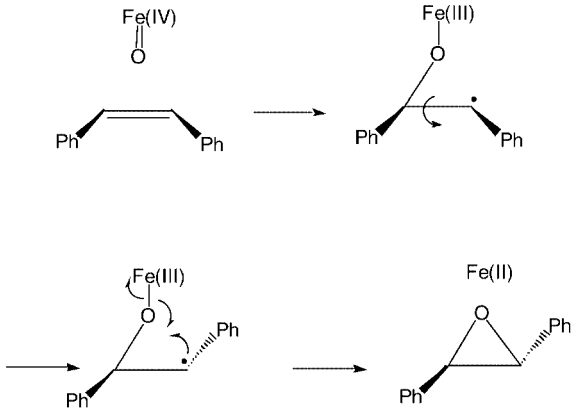

Scheme 3

With the different substrates, the same experiments performed at 20 °C did not lead to any oxidation products even in the presence of a higher ClO^- concentration. This indicates that ClO^- is not directly responsible for these oxidations. This remark is important since hypochlorite may exhibit an oxidation activity in the presence of Lewis-acidic species.[53] Moreover, at room temperature, the solution became rapidly colorless and a reddish solid precipitated which is very likely to be iron oxide as suggested by Mössbauer spectroscopy (see above). On the contrary, after 2 h at −20 °C, the solution was still yellow and only a small amount of solid was observed.

This reactivity in acetonitrile/dichloromethane strongly supports the presence of a $[L_5{}^3Fe^{IV}O]^{2+}$ species.

As pointed out by Lim et al.,[26] the reactivity of $Fe^{IV}=O$ species appears to correlate strongly with their stability:

the less stable the species, the stronger the oxidant. The complex $[Fe^{IV}(O)(TMC)(NCCH_3)]^{2+}$, which is stable for at least one month at −40 °C, is capable of oxidizing PPh_3 but not olefins.[25] The TPA complex[26] and the porphyrin analog $[Fe^{IV}(O)(TMP)]$,[52] which are less stable than the former, are able to epoxidize olefins. The $L_5{}^3$ complex, which is much more unstable than the above complexes, is also much more reactive since it is even able to hydroxylate unactivated C−H bonds.

Quantum Calculations

The value of the molar extinction coefficient (300 $M^{-1}\cdot cm^{-1}$) of the band observed at 742 nm in methanol seems low when compared with the intense bands which have been recently detected in the 500−900-nm region for the low-spin $Fe^{IV}{}_2O_2$ model system described by Costas et al.[18] On the contrary it agrees well with the value of 400 $M^{-1}\cdot cm^{-1}$ observed at 820 nm for the X-ray characterized non-heme complex $[Fe^{IV}(O)(TMC)(NCCH_3)]^{2+}$.[25]

Spin-unrestricted DFT calculations were performed on the model compounds $[(NH_3)_5Fe^{IV}O]^{2+}$ and $[(NH_3)_5Fe^{IV}OCH_3]^{3+}$ as well as on the real complex $[L_5{}^3Fe^{IV}O]^{2+}$ using the Gaussian98 program package[54] with Becke's three parameter hybrid functional[55] and the correlation functional of Lee, Yang and Parr (B3LYP).[56] For both models, atomic distances were optimized in the two $S = 1$ and $S = 2$ spin states leading to the conclusion that the low-spin state is the more stable. The geometry of the real complex was fully optimized only in the $S = 1$ spin state. For the oxo model, the Fe−O bond length was found to be 1.635 Å, consistent with the value reported by Lehnert et al.[57,58]

The electronic absorption spectrum of the model compound $[(NH_3)_5Fe^{IV}O]^{2+}$ in the low-spin state ($S = 1$) was computed by time-dependent DFT (TDDFT) (see Exp. Sect.). It shows in the visible region only one weak band at 600 nm (oscillator strength $f = 0.0015$) (see Supporting Information). In C_{4v} symmetry (z being the Fe−O axis) this band corresponds to two degenerate transitions. The first one, with y polarization, consists of approximately equal amounts of an α excitation from the antibonding $d_{yz} - p_y$ orbital to a $d_{x^2-y^2}$-type orbital and of a β excitation from a d_{xy}-type orbital to the antibonding $d_{xz} - p_x$ orbital. The second one is the corresponding x-polarized transition involving excitation from the α-antibonding $d_{xz} - p_x$ orbitals to $d_{x^2-y^2}$ and β excitation from d_{xy} to the antibonding $d_{yz} - p_y$ orbital. These two transitions have therefore both MLCT and LMCT character. As a consequence, no appreciable charge transfer occurs and the observed band is essentially a weak-intensity d−d transition. This calculation then confirms the explanation proposed by Rohde et al. to interpret the observed low intensity.[25] The expected oxo-to-Fe^{IV} LMCT band was found at 360 nm with z polarization and involves β transitions from bonding $d_{xz} + p_x$ to antibonding $d_{xz} - p_x$ orbitals and from bonding $d_{yz} + p_y$ to antibonding $d_{yz} - p_y$ orbitals (see Supporting Information).

These conclusions can be compared with those we obtained for the Fe^{IV}−methoxo system $[(NH_3)_5Fe^{IV}OCH_3]^{3+}$. The geometry optimization led to a linear Fe−O−CH_3 motif with a short Fe−O distance of 1.709 Å, only slightly larger than the value of 1.635 Å found for the oxo model. In this case, however, the MOs containing the p_x and p_y contributions of oxygen delocalized on the CH_3 group and two essentially d−d transitions were calculated at 550 (d_{xz} or d_{yz} to d_{z^2}) and 450 nm (d_{xz} or d_{yz} to $d_{x^2-y^2}$) ($f \approx 0.0015$). The former had a zero intensity in the oxo model (see Supporting Information). The full geometry optimization of the real complex $[L_5{}^3Fe^{IV}O]^{2+}$ in the $S = 1$ state gave an Fe−O distance of 1.646 Å. In the visible region (see Supporting Information), the computed spectrum exhibits a band at 530 nm ($\varepsilon = 500\ M^{-1}.cm^{-1}$) which results from nondegenerate transitions essentially from d_{xz}- or d_{yz}-type orbitals to a $d_{x^2-y^2}$-type orbital. The LMCT transition from bonding $d + p_O$ to antibonding $d - p_O$ orbitals was calculated at 382 nm. We stress the fact that most of the informations relative to the calculated spectrum of the real complex were present in the simple model and that all orbitals of concern are strikingly similar, except for a small delocalization on the ligand $L_5{}^3$.

Finally, these calculations indicate that the weak band observed at 742 nm in MeOH for this low-spin Fe^{IV} mononuclear species has predominantly d−d character.

We would like to finish this part with some simple theoretical considerations. Is the Fe^{IV}=O notation the most accurate for a ferryl species? As is well known, the basic theoretical description of an $S = 1$ low-spin Fe^{IV}=O motif implies MOs combining the "t_{2g}" d orbitals with the p_x and p_y O orbitals to give occupied π-bonding orbitals and semi-occupied π*-antibonding orbitals with $\pi_x^* = \lambda\ d_{xz} + \mu\ p_x$ and $\pi_y^* = \lambda\ d_{yz} + \mu\ p_y$ as illustrated in Scheme 4.

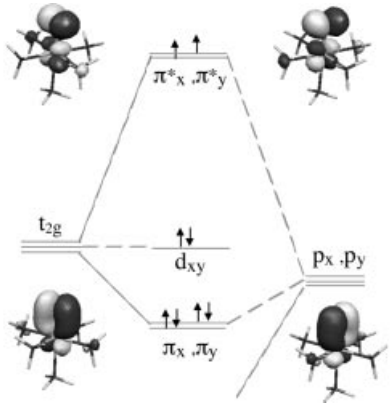

Scheme 4

This MO description enables us to understand both the delocalized spin triplet character and the double bond composed of a σ bond (not shown) and two half π bonds.

It is instructive to examine the electronic structure of $Fe^{IV}O$ from a Valence Bond point of view. The triplet state is represented by the following Slater determinant:

$$|\pi_x^*\ \pi_y^*| = \lambda^2\,|d_{xz}\ d_{yz}| + \lambda\mu\,|d_{xz}\ p_y| + \lambda\mu\,|p_x\ d_{yz}| + \mu^2\,|p_x\ p_y|$$

The determinant $|d_{xz}\ d_{yz}|$ describes a spin triplet localized on Fe in an $Fe^{IV}{}_{LS}-O^-$ pair, the $|d_{xz}\ p_y|$ and $|p_x\ d_{yz}|$ ones describe spin triplets equally shared between Fe and O in an $Fe^{III}{}_{LS}-O^\circ$ pair and the $|p_x\ p_y|$ one describes a spin triplet localized on O in an $Fe^{II}{}_{LS}-O^{\circ\circ+}$ pair. The electron distributions related to these mesomeric forms in the ground state are represented in part a) of Scheme 5.

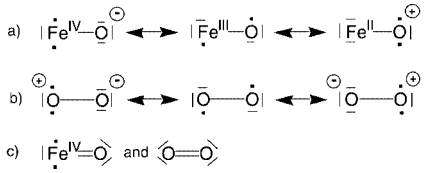

Scheme 5. In a) all forms have an actual charge of +2; the formal oxidation states are reported for Fe and the formal charges for O

Making the simplifying assumption of zero overlap between the d and p orbitals for this qualitative discussion, we deduced from the wave function $|\pi_x^*\ \pi_y^*|$ that the weight is λ^4 for the $Fe^{IV}-O^-$ form, μ^4 for the $Fe^{II}{}_{LS}-O^{\circ\circ+}$ and $2\lambda^2\mu^2$ for the $Fe^{III}{}_{LS}-O^\circ$ form, with $\lambda^2 + \mu^2 = 1$ arising from the normalization conditions of π_x^* and π_y^*. Within the same assumption of zero overlap, the spin densities are $\rho_{Fe} = 2\,\lambda^2$ and $\rho_O = 2\,\mu^2$. Scheme 6 represents the weight of each different mesomeric form as a function of μ^2.

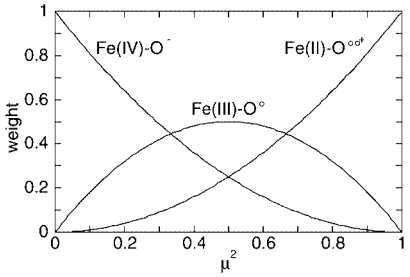

Scheme 6

The DFT calculations showed that the spin density is in fact almost equally shared between iron and oxygen, as shown in Figure 4. Within our simple hypothesis, this would imply $\lambda^2 \approx \mu^2$. When $\lambda^2 = \mu^2 = 0.5$, the $Fe^{IV}-O^-$ form amounts to 25%, the $Fe^{III}{}_{LS}-O^\circ$ form to 50% and the $Fe^{II}{}_{LS}-O^{\circ\circ+}$ form to 25%. When μ^2 decreases slightly from 0.5, the amount of $Fe^{II}{}_{LS}-O^{\circ\circ}$ evidently decreases whereas the amount of the $Fe^{IV}-O^-$ form increases. The Fe^{IV} orbitals are lowered so much in energy that they become close to the oxygen p orbitals which themselves are destabilized in O^{2-}. These AOs interact strongly and the MOs are delocalized on both Fe and O as reflected in the short Fe−O distance. The simple model of zero overlap no longer holds, but it allows us to conclude that the system has gained a significant $Fe^{III}{}_{LS}-O^\circ$ character and even $Fe^{II}{}_{LS}-O^{\circ\circ}$ character.

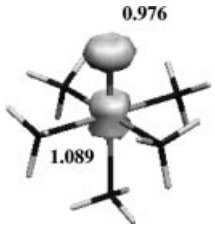

Figure 4. Spin densities calculated for the model compound $[(NH_3)_5Fe^{IV}O]^{2+}$

The description of the "$Fe^{IV}O$" species simultaneously as a diradical and a double bond system is in fact reminiscent of the electronic structure of the dioxygen molecule. It has also to be noted that, for the compound I of cytochrome P-450, the iron−oxo moiety possesses a triplet pair of electrons in π* orbitals.[59] For dioxygen the different forms are represented in part b) of Scheme 5. It is evident from symmetry that the spin is equally distributed on both oxygen atoms in triplet dioxygen. As explained by Valence Bond theory,[60] the double-bond character of O_2 arises from one σ bond, half a π_x bond and half a π_y bond and is fully compatible with a triplet state.

As represented in part c) of Scheme 5, the double-bond notation is unsatisfying both for $Fe^{IV}O$ and O_2 since this notation masks the spin density on the oxygen atom(s).

At this stage we stress that the $Fe^{III}{}_{LS}-O^\circ$ mesomeric form is dominant in the low spin ferryl system and, as for O_2, the strong radical character on O may explain the reactivity observed (see above).

We went beyond the monodeterminantal representation of the $S = 1$ ferryl ground state. We have performed a self consistent field computation (SCF) with full Configuration Interaction (CI) involving the subset of π and π* orbitals (complete active-space multi configuration SCF/CASSCF) together with localization of these orbitals into orthogonal orbitals with predominant p_x, p_y, d_{xz} and d_{yz} character. This procedure gave us the following contributions for each form: $Fe^{III}{}_{LS}-O^\circ \approx 94.5\%$, $Fe^{II}{}_{LS}-O^{\circ\circ+} \approx 5\%$ and $Fe^{IV}-O^-$ only $\approx 0.5\%$. This enrichment in $Fe^{III}{}_{LS}-O^\circ$ form is related to the removal of charge fluctuation by CI.[61] Basically, in the $Fe^{III}{}_{LS}-O^\circ$ form the monocenter electron−electron repulsion is weakened. Similarly, CI for O_2 leads to more than 80% diradical form.[62]

Conclusion

In MeOH at low temperature, we have obtained green intermediates, after reaction of XO^- (X = Cl, Br) and Fe^{II} complexes bearing the pentadentate amine/pyridine ligands $L_5{}^3$ or $L_5{}^2$. These green complexes have been assigned as Fe^{IV} entities, i.e. $[LFe^{IV}O]^{2+}$ or possibly $[LFe^{IV}OCH_3]^{3+}$ if the former reacts with MeOH. To date, $[LFe^{IV}O]^{2+}$ or $[L_5{}^3Fe^{IV}OCH_3]^{3+}$ complexes are among the first non-heme Fe^{IV} mononuclear species characterized. Spectroscopic

studies are underway to determine which of the two possible formulations of the species is occurring in MeOH.

The reactivity, performed in acetonitrile/dichloromethane solution showed that the $ClO^-/L_5{}^3$ system is able to oxidize cyclohexane to cyclohexanol as well as cyclooctene and *cis*-stilbene to the corresponding epoxides although in the last case with a complete isomerization to the *trans* form. These very specific oxidations are consistent with the mediation of a ferryl intermediate. Moreover, we have performed DFT calculations and obtained the electronic description of the ground state for the triplet "$Fe^{IV}O$" complex. As for the triplet dioxygen molecule, the ferryl−oxo complex is actually better described as the diradical $Fe^{III}-O^{\circ}$ form. This strong radical character on the oxygen atom must be at the origin of the hydroxylation and epoxidation reactivity, in particular the isomerization observed during oxidation of the *cis*-stilbene.

Experimental Section

Materials: Starting materials were purchased from Acros. Solvents were purchased from Merck and used without further purification.

Syntheses

Ligand *N*-Methyl-*N*,*N*′,*N*′-tris(2-pyridylmethyl)ethane-1,2-diamine ($L_5{}^2$): This ligand was synthesized according to the method reported by Bernal et al.[27]

Ligand *N*-Methyl-*N*,*N*′,*N*′-tris(2-pyridylmethyl)propane-1,3-diamine ($L_5{}^3$): This ligand was obtained according to the method reported by Bernal et al.[27] using *N*-methylpropane-1,3-diamine as the starting material. The crude product obtained after evaporation of $CHCl_3$ was a dark oil purified by chromatography on Al_2O_3 (eluent $CHCl_3$/EtOH, 20:1).

Complex $[L_5{}^2Fe^{II}Cl]PF_6$: This complex was obtained as described previously.[27]

Complex $[L_5{}^3Fe^{II}Cl]PF_6$: The method described by Balland et al.[36] has been reproduced here.

^{18}O-Labelled BrO^-: ^{18}O-labelled BrO^- was prepared using $H_2{}^{18}O$ (purchased from Eurisotop, isotopic enrichment 95%) according to the method reported by Bortolini et al.[63]

Reactivity Experiments: Reactivity experiments were performed at −20 °C in CH_3CN/CH_2Cl_2, 1:1, under vigorous stirring. The amounts of reactants were: 10^{-3} mmol of Fe complex; 2 equiv. of ClO^-, and 800 equiv. of substrate. The oxidation products were analyzed by GC. The conversion of *cis*-stilbene into the *trans*-epoxide was determined by NMR spectroscopy.

Physical Measurements: UV/Vis spectra were recorded with a Varian Cary 5E spectrophotometer equipped with a Dewar fitted with quartz windows for low-temperature measurements. Stopped-flow experiments were performed with a Biologic SFM-300 instrument equipped with a Julabo F 30C cryostat. Spectra were recorded in the 200−1022-nm range with a 0.5-cm optical path and a 50-μL cuvette. The delay after mixing was 3 ms. Mössbauer data were recorded with an alternating constant-acceleration spectrometer. The minimum experimental line width was 0.24 mm·s^{-1} (full width at half-height). The sample temperature was maintained at a constant value either with an Oxford Instruments Variox or an Oxford Instruments Mössbauer-Spectromag cryostat. The latter is a split-pair superconducting magnet system for applied fields up to 8 T where the temperature of the sample can be varied in the range of 1.5−250 K. The field at the sample is perpendicular to the γ-beam. The ^{57}Co/Rh source (1.8 GBq) was positioned at room temperature inside the gap of the magnet system at a zero-field position. Isomer shifts are quoted relative to iron metal at 300 K. Samples were doped at 50% with ^{57}Fe. The solutions were prepared at −60 °C in MeOH (5.5 mM in Fe) and were studied at 77 K. Resonance Raman spectra were recorded using a Jobin Yvon spectrometer equipped with a 900 lines/mm grating and a liquid-nitrogen cooled CCD camera. The 752.5-nm line of a Kr^+ laser was used for excitation with a power of 50 mW. The samples (1.5 mM in iron) were prepared at −80 °C in CH_3OH/acetone, 2:1, then frozen and studied at 10 K.

Computational Details: Spin-unrestricted DFT calculations were performed on the model compounds $[(NH_3)_5Fe^{IV}O]^{2+}$ and $[(NH_3)_5Fe^{IV}OCH_3]^{3+}$ as well as on the real complex $[L_5{}^3Fe^{IV}O]^{2+}$ using the Gaussian98 program package[54] with Becke's three parameter hybrid functional[55] and the correlation functional of Lee, Yang and Parr (B3LYP).[56] The double zeta basis set (SV) of Ahlrichs et al.[64] was employed for all atoms. For both models the distances were optimized in the two $S = 1$ and $S = 2$ spin states leading to the conclusion that the low-spin state is the more stable and the geometry of the complex was fully optimized in the $S = 1$ spin state. The energy of the excited states and oscillator strengths, *f*, were calculated by the Time Dependent DFT (TDDFT) formalism as implemented in the Gaussian98 program.[65] The theoretical electronic spectra were then simulated using Gaussian line shapes with a bandwidth at half-height of 2000 cm^{-1}, a value which usually gives molar extinction coefficients consistent with experimental values. For the configuration interaction calculations, Slater-type orbitals (STO-3G) were used.[66]

Supporting Information: Energy diagram and contour plot of the molecular orbitals calculated by DFT for the model complex $[(NH_3)_5Fe^{IV}O]^{2+}$ in the $S = 1$ state (Figure S1). Theoretical UV/Vis spectra of the models $[(NH_3)_5Fe^{IV}O]^{2+}$ and $[(NH_3)_5Fe^{IV}OCH_3]^{+}$ and of the real complex $[L_5{}^3Fe^{IV}O]^{2+}$ (Figures S2, S3, S4, respectively).

[1] T. H. Moss, A. Ehrenberg, A. J. Bearden, *Biochemistry* **1969**, *8*, 4159.
[2] C. E. Schulz, P. W. Devaney, H. Winkler, P. G. Debrunner, N. Doan, R. Chiang, R. Rutter, L. P. Hager, *FEBS Lett.* **1979**, *103*, 102.
[3] C. E. Schulz, R. Rutter, J. T. Sage, P. G. Debrunner, L. P. Hager, *Biochemistry* **1984**, *23*, 4743.
[4] J. Terner, A. J. Sitter, C. M. Reczek, *Biochim. Biophys. Acta* **1985**, *828*.
[5] A. J. Sitter, C. M. Reczek, J. Terner, *Biochim. Biophys. Acta* **1985**, *828*, 229.
[6] S. Hashimoto, J. Teraoka, T. Inubushi, T. Yonetani, T. Kitagawa, *J. Biol. Chem.* **1986**, *261*, 11110.
[7] T. Uchida, M. Tatsushi, T. Kitagawa, *Biochemistry* **2000**, *39*, 6669.
[8] M. Schappacher, G. Chottard, R. Weiss, *J. Chem. Soc., Chem. Commun.* **1986**, 93.
[9] D. Mandon, R. Weiss, K. Jayaraj, A. Gold, J. Terner, E. Bill, A. X. Trautwein, *Inorg. Chem.* **1992**, *31*, 4404.
[10] K. Jayaraj, A. Gold, R. N. Austin, L. M. Ball, J. Terner, D. Mandon, R. Weiss, J. Fischer, A. DeCian, E. Bill, M. Müther, V. Schünemann, A. X. Trautwein, *Inorg. Chem.* **1997**, *36*, 4555.
[11] J. Terner, A. Gold, R. Weiss, D. Mandon, A. X. Trautwein, *J. Porphyrins Phthalocyanines* **2001**, *5*, 357.

[12] L. Shu, J. Nesheim, K. Kauffmann, E. Münck, J. D. Lipscomb, L. Que, *Science* **1997**, *275*, 515.
[13] B. E. Sturgeon, D. Burdi, S. Chen, B. H. Huynh, D. E. Edmonson, J. Stubbe, B. M. Hoffman, *J. Am. Chem. Soc.* **1996**, *118*, 7551.
[14] Y. Dong, L. Que, K. Kauffmann, E. Münck, *J. Am. Chem. Soc.* **1995**, *117*, 11377.
[15] Y. Dong, Y. Zang, L. Shu, E. C. Wilkinson, L. Que, K. Kauffmann, E. Münck, *J. Am. Chem. Soc.* **1997**, *119*, 12683.
[16] D. Lee, J. L. DuBois, B. Pierce, D. Petasis, M. P. Hendrich, C. Krebs, B. H. Huynh, S. J. Lippard, *J. Am. Chem. Soc.* **1999**, *121*, 9893.
[17] H.-F. Hsu, Y. Dong, L. Shu, V. G. Young, L. Que, *J. Am. Chem. Soc.* **1999**, *121*, 5230.
[18] M. Costas, J.-U. Rohde, A. Stubna, R. Y. N. Ho, L. Quaroni, E. Münck, L. Que, *J. Am. Chem. Soc.* **2001**, *123*, 12931.
[19] N. I. Burzlaff, P. J. Rutledge, I. J. Clifton, C. M. H. Hensgens, M. Pickford, R. M. Adlington, P. L. Roach, J. E. Baldwin, *Nature* **1999**, *401*, 721.
[20] Z. H. Zhang, J. S. Ren, D. K. Stammers, J. E. Baldwin, K. Harlos, C. J. Schofield, *Nat. Struct. Biol.* **2000**, *7*, 127.
[21] H. Miyake, S. J. Lange, L. Que, *Inorg. Chem.* **2001**, *40*, 3534.
[22] K. L. Kostka, B. G. Fox, M. P. Hendrich, T. J. Collins, L. J. Rickard, L. J. Wright, E. Münck, *J. Am. Chem. Soc.* **1993**, *115*, 6746.
[23] M. J. Bartos, S. W. Gordon-Wylie, B. G. Fox, L. J. Wright, S. T. Weintraub, K. Kauffmann, E. Münck, K. L. Kostka, E. S. Uffelman, C. E. F. Rickard, K. R. Noon, T. J. Collins, *Coord. Chem. Rev.* **1998**, *174*, 361.
[24] C. A. Grapperhauser, B. Mienert, E. Bill, T. Weyhermüller, K. Wieghardt, *Inorg. Chem.* **2000**, *39*, 5306.
[25] J. U. Rohde, J. H. In, M. H. Lim, W. W. Brennessel, M. R. Bukowski, A. Stubna, E. Munck, W. Nam, L. Que, *Science* **2003**, *299*, 1037.
[26] M. H. Lim, J. U. Rohde, A. Stubna, M. R. Bukowski, M. Costas, R. Y. N. Ho, E. Munck, W. Nam, L. Que, *Proc. Natl. Acad. Sci. USA* **2003**, *100*, 3665.
[27] I. Bernal, I. M. Jensen, K. B. Jensen, C. J. McKenzie, H. Toftlund, J. P. Tuchagues, *J. Chem. Soc., Dalton Trans.* **1995**, 3667.
[28] M. Lubben, A. Meetsma, E. C. Wilkinson, B. Feringa, L. Que, *Angew. Chem. Int. Ed. Engl.* **1995**, *34*, 1512.
[29] M. E. deVries, R. M. LaCrois, G. Roelfes, H. Kooijman, A. L. Spek, R. Hage, B. L. Feringa, *Chem. Commun.* **1997**, 1549.
[30] P. Mialane, A. Novorojkine, G. Pratviel, L. Azéma, M. Slany, F. Godde, A. Simaan, F. Banse, T. Kargar-Grisel, G. Bouchoux, J. Sainton, O. Horner, J. Guilhem, L. Tchertanova, B. Meunier, J. J. Girerd, *Inorg. Chem.* **1999**, *38*, 1085.
[31] A. J. Simaan, F. Banse, P. Mialane, A. Boussac, S. Un, T. Kargar-Grisel, G. Bouchoux, J. J. Girerd, *Eur. J. Inorg. Chem.* **1999**, 993.
[32] K. B. Jensen, C. J. McKenzie, L. P. Nielsen, J. Z. Pedersen, H. M. Svendsen, *Chem. Commun.* **1999**, 1313.
[33] R. Y. N. Ho, G. Roelfes, B. L. Feringa, L. Que, *J. Am. Chem. Soc.* **1999**, *121*, 264.
[34] G. Roelfes, M. Lubben, K. Chen, R. Y. N. Ho, A. Meestma, S. Genseberger, R. M. Hermant, R. Hage, S. K. Mandal, V. G. Young, Y. Zang, H. Kooijman, A. L. Spek, L. Que, B. L. Feringa, *Inorg. Chem.* **1999**, *38*, 1929.
[35] J. J. Girerd, F. Banse, A. J. Simaan, *Struct. Bond.* **2000**, *97*, 146.
[36] V. Balland, F. Banse, E. Anxolabéhère-Mallart, M. Ghiladi, T. Mattioli, C. Philouze, G. Blondin, J.-J. Girerd, *Inorg. Chem.* **2003**, *42*, 2470.
[37] N. N. Greenwood, T. C. Gibb, *Mössbauer Spectroscopy*, Chapman and Hall Ltd., London, **1971**.
[38] E. Münck, in *Physical Methods in Bioinorganic Chemistry* (Ed.: L. Que), University Science Books, Sausalito, California, **2000**.
[39] A. X. Trautwein, E. Bill, E. Bominaar, H. Winkler, *Struct. Bond.* **1991**, *78*, 1.
[40] D. Lee, B. Pierce, C. Krebs, M. P. Hendrich, B. H. Huynh, S. J. Lippard, *J. Am. Chem. Soc.* **2002**, *124*, 3993.
[41] H. Zheng, S. J. Yoo, E. Munck, L. Que, *J. Am. Chem. Soc.* **2000**, *122*, 3789.
[42] J. T. Groves, R. Quinn, T. J. McMurry, G. Lang, B. Boso, *J. Chem. Soc., Chem. Commun.* **1984**, 1455.
[43] J. T. Groves, R. Quinn, T. J. McMurry, M. Nakamura, G. Lang, B. Boso, *J. Am. Chem. Soc.* **1985**, *107*, 354.
[44] T. J. Collins, B. G. Fox, Z. G. Hu, K. L. Kostka, E. Münck, C. E. F. Rickard, L. J. Wright, *J. Am. Chem. Soc.* **1992**, *114*, 8724.
[45] W. A. Oertling, R. T. Kean, R. Wever, G. T. Babcock, *Inorg. Chem.* **1990**, *29*, 2633.
[46] S. Hashimoto, Y. Tatsuno, T. Kitagawa, *Proc. Natl. Acad. Sci. USA* **1986**, *83*, 2417.
[47] B. Meunier, J. Bernadou, *Struct. Bond.* **2000**, *97*, 1.
[48] B. Meunier, *Chem. Rev.* **1992**, *92*, 1411.
[49] R. Weiss, A. Gold, A. X. Trautwein, J. Terner, *The Porphyrin Handbook*, Academic Press, San Diego, **2000**, vol. *4*, p. 72.
[50] Y. Watanabe, H. Fujii, *Struct. Bond.* **2000**, *97*, 59.
[51] M. Costas, K. Chen, L. Que, *Coord. Chem. Rev.* **2000**, *200−202*, 517.
[52] J. T. Groves, Z. Gross, M. K. Stern, *Inorg. Chem.* **1994**, *33*, 5065.
[53] W. Nam, J. S. Valentine, *J. Am. Chem. Soc.* **1990**, *112*, 4977.
[54] M. J. Frisch, G. W. Trucks, H. B. Schlegel, G. E. Scuseria, M. A. Robb, J. R. Cheeseman, V. G. Zakrzewski, J. A. Montgomery, Jr., R. E. Stratmann, J. C. Burant, S. Dapprich, J. M. Millam, A. D. Daniels, K. N. Kudin, M. C. Strain, O. Farkas, J. Tomasi, V. Barone, M. Cossi, R. Cammi, B. Mennucci, C. Pomelli, C. Adamo, S. Clifford, J. Ochterski, G. A. Petersson, P. Y. Ayala, Q. Cui, K. Morokuma, D. K. Malick, A. D. Rabuck, K. Raghavachari, J. B. Foresman, J. J. V. Cioslowski, A. G. Ortiz, B. B. Baboul, G. Stefanov, A. Liu, Liashenko, P. Piskorz, I. Komaromi, R. Gomperts, R. L. Martin, D. J. Fox, T. Keith, M. A. Al-Laham, C. Y. Peng, A. Nanayakkara, C. Gonzalez, M. Challacombe, P. M. W. Gill, B. Johnson, W. Chen, M. W. Wong, J. L. Andres, C. Gonzalez, M. Head-Gordon, E. S. Replogle, J. A. Pople, *Gaussian 98*, Gaussian, Inc., Pittsburgh PA, **1998**.
[55] A. D. Becke, *J. Chem. Phys.* **1993**, *98*, 5648.
[56] C. Lee, W. Yang, R. G. Parr, *Phys. Rev. B* **1988**, *37*, 785.
[57] N. Lehnert, R. Y. N. Ho, L. Que, E. I. Solomon, *J. Am. Chem. Soc.* **2001**, *123*, 8271.
[58] N. Lehnert, F. Neese, R. Y. N. Ho, L. Que, E. I. Solomon, *J. Am. Chem. Soc.* **2002**, *124*, 10810.
[59] S. Shaik, S. P. de Visser, F. Ogliaro, H. Schwarz, D. Schroder, *Curr. Opin. Chem. Biol.* **2002**, *6*, 556.
[60] P. C. Hiberty, *J. Mol. Struct.: Theochem* **1998**, *451*, 237−261.
[61] J.-P. Malrieu, in *Valence Bond Theory and Chemical Structure*, vol. 64 (Eds.: D. J. Klein, N. Trinajstic), Elsevier, Amsterdam, Oxford, New York, Tokyo, **1990**.
[62] L. Salem, *Electrons in Chemical Reactions − First Principles*, Wiley-Interscience, **1982**.
[63] O. Bortolini, M. Ricci, B. Meunier, P. Friant, I. Ascone, J. Goulon, *New. J. Chem.* **1986**, *10*, 39.
[64] A. Schaefer, H. Horn, R. Ahlrichs, *J. Chem. Phys.* **1992**, *97*, 2571.
[65] M. E. J. Casida, K. C. Casida, D. R. Salahub, *J. Chem. Phys.* **1998**, *108*, 4439.
[66] W. J. Hehre, R. F. Stewart, J. A. Pople, *J. Chem. Phys.* **1969**, *51*, 2657.

Received May 16, 2003
Early View Article
Published Online November 20, 2003

